

## Initial Studies for AE Characterisation of Damage in Composite Materials

Venturini Autieri, M. R. and Dulieu-Barton, J. M.

School of Engineering Sciences, University of Southampton, Southampton SO15 5BY, UK  
[mva@soton.ac.uk](mailto:mva@soton.ac.uk), [janice@ship.soton.ac.uk](mailto:janice@ship.soton.ac.uk)

**Keywords:** Acoustic emission, Carbon Fibre Reinforced Polymer (CFRP), characterisation, pencil lead breaks (PLBs).

**Abstract.** Some initial studies for an AE characterisation of damage in composites are presented in this paper. A PAC AE PCI-2 based system and four PAC WD AE broadband sensors are used. Pencil lead breaks (PLB) were used to introduce a source of elastic waves. An initial validation of the system based on PLB on an aluminium plate showed that there was a large difference in sensitivity of the four nominally identical sensors. It is shown that the AE parameters are so strongly related to the sensitivity of the sensors that they tend to describe the AE system more than the actual sources. To characterise damage in composite materials alternative AE parameters are required that are not dependent on the sensitivity of the sensors. In the paper, it is shown that the frequency spectra of the sources have relatively little variability with respect to the sensor. A frequency-based approach that examines the spectrum of each source is proposed in the paper. The procedure is demonstrated using PLBs on a CFRP plate and it is demonstrated that the approach can indicate the position of the source in relation to orientation of the fibres and the plate edge.

### Introduction

Acoustic Emission (AE) characterisation of damage in CFRP is an active research field, and several works have been produced, that aim to identify some characteristic features within the acoustic emissions in terms of AE parameters (de Groot et al., 1995, Huguet, et al., 2002, Woo et al. 2004) or waveforms (Bohse, 2000, Ferreira et al., 2004, Johnson and Gudmunson, 2001, Johnson and Gudmunson, 2000, Mizutani et al., 2000). In (de Groot et al., 1995) and (Woo et al., 2004) the authors attempt to assign a frequency range within which the damage occurs. In (Huguet, et al., 2002) a Kohonen map is devised using from the acoustic emission using a neural network approach. This allowed two types of emission to be identified that occurred at different times during the loading of tensile specimens with different fibre orientations and indicated that the emission type may be related to the damage type. In (Bohse, 2000) epoxy resin samples, single carbon fibres embedded in epoxy resin and actual multi-fibre specimens are examined both in tension and in mode 1 fracture through a double cantilever beam specimen. It is shown that there is some correlation between AE features and the stress strain history of the materials. However the most important feature of this work in relation to the current paper is the use of average power spectra to characterise different types of sources. Ferreira et al (2004) provide a visual representation of typical spectra obtained from glass/epoxy specimens and use wavelet transforms to associate frequency spectra groups with the failure modes. In (Johnson and Gudmunson, 2001, Johnson and Gudmunson, 2000) the authors use sensors mounted on either side of a tensile specimen in an attempt to decouple the extensional and flexural waves, they also highlight that the measurement of strain rather than load is important and that the smaller the sensor the better the results. In (Mizutani et al., 2000) sources were generated in CFRP under compressive loading from various types of internal damage and these were compared with simulated sources induced using a laser. It was shown that the sources could be classified into four types using their frequency spectra and wavelet transforms. It is clear that there has been significant research effort devoted to AE characterisation of damage in composite materials; however such characterisation is still far from being definitive. The commonality in virtually all the work is the overarching assumption is that the characteristic features derived from the AE depend exclusively on the originating damage (i.e. fibre breakage,

matrix cracking, delamination, fibre pull-out). A study of the theory of elastic waves (Auld, 1973) shows that this is not the case and the signal from the sensor will be dependent on the path of the source. Clearly in orthotropic layered inhomogeneous media such as CFRP the source path is a major consideration.

In the current work it was intended to adopt some of the procedures described in (Johnson and Gudmunson, 2001, Johnson and Gudmunson, 2000) above. However preliminary work showed that the nominally identical sensors that were supplied responded differently to practically identical sources. Therefore it was decided to carry out some validation and sensitivity tests to assess the effect of the sensor response on the AE features. In this article, the analysis of the results from two experiments with PLB will be presented, to investigate: (i) the effectiveness of a pure AE-parameters approach for a characterisation of the source, (ii) if the same sources originating from and travelling through a same medium give consistent and “typical” AE signals. After the first task, source characterisation based on standard AE parameters (e.g. counts, duration, amplitude) was eliminated as a means for damage identification. For the second task, several PLB carried out on a unidirectional carbon/epoxy composite panel were examined in detail using a frequency-based approach. The effect of the orientation of the fibres and the proximity to the edges of the specimens on the transmission and detection of the acoustic emissions was studied. The results indicated that any characterisation of a source must account for the material under investigation and the component geometry. This is discussed in detail in the paper focusing on the implications for damage characterisation in composites using AE.

### **AE system and sensors**

The AE system used in this research was manufactured by Physical Acoustic Corporation, USA. It includes two PAC PCI-2 boards for a total of four AE channels, which are referred to as C1, C2, C3 and C4 throughout this work. Four PAC “2/4/6” pre-amplifiers were used in the work and these were labelled P1, P2, P3 and P4. The sensors used in this work are four nominally identical wideband PAC WD, chosen because the frequency range of the acoustic emissions reported in literature, e.g. de Groot et al. (1995) and Woo et al. (2004) occur over a large spectrum. The sensors, with serial numbers AJ51, AJ49, AJ57, AJ60, were respectively labelled as S1, S2, S3, and S4. The documented characteristics the four sensors are provided by the manufacturer in the form of calibration curves of sensitivity in dB against frequency. A comparison of the curves for the four sensors was done by superimposing the curves obtained from their calibration certificates into one plot as shown in Fig. 1. This shows that the curves for the nominally identical sensors differ considerably and that at certain frequencies the difference is as great as 10 dB. The plot shown in Fig. 1 is divided into three frequency ranges labelled as A (ranging up to 300 kHz), B (covering from 300 to 650 kHz) and C (over 650 kHz). Although the AE from composite materials is broadband the literature indicates that most of the activity occurs at frequencies in the range covering regions A and B. It is clear from Fig. 1 that the response of the sensors differs in these regions. In A the response of S2 differs from the most from the other sensors, although at approximately 0.28 MHz there is a peak in the response of S3 and S4 that is not evident in the other sensors. In region B the response of S3 and S4 is practically identical, however the response S1 is around 5 dB less and S2 10 dB less. Interestingly, across the spectrum shown in Fig. 1, the order of the four sensors sensitivities is not the same. The wide variation in the response of the sensors must have some effect on the results particularly the calculated hit/absolute energy and other AE features. Therefore series of experiments were designed to establish the effect this variability had on the results and on the frequency spectrum. It should be noted that these differences in sensitivity cannot be adjusted by preamplification as the sensors are broadband and have a non-uniform frequency response.

### General experimental and analysis procedure

In all the tests described in this paper all the AE sources were generated by PLBs in a different manner to the standard Hsu-Nielsen source. The breaks were produced by leaning the pencil onto the surface and then rotating the pencil around the pivotal point of contact with the surface; this procedure was developed as it to minimised the noise produced by the impact of the Teflon guide on the specimen (as in a standard calibration). It should be noted that the Hsu-Nielsen source was chosen as standard as it is able to produce consistent results in terms of “amplitude,” but not necessarily of frequency spectrum. The modified procedure was adopted to achieve a better uniformity in the frequency.

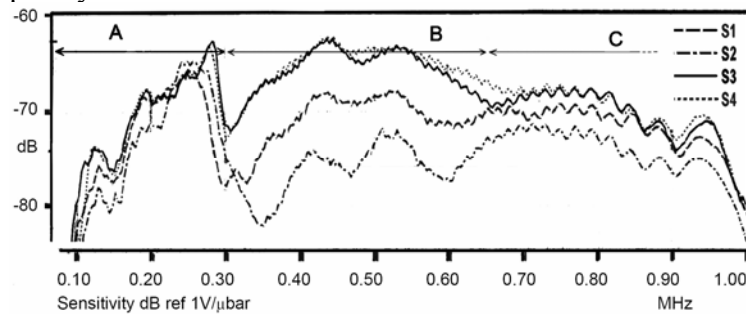


Fig. 1. Sensor calibration certificates superimposed

For the analysis of the data, PAC AEWIn 1.56 software was used in conjunction with some Matlab code for producing the average frequency spectra from exported waveforms. In the results, for the AE parameters data, the arithmetic mean is shown, whereas for the waveforms, the power spectra are calculated as the geometric mean of all the considered spectra, together with the average frequency centroids of all the spectra.

### Influence of the sensor response on the AE features

**Testing setup.** The first tests involved all the four sensors mounted onto an aluminium plate ( $350 \times 250 \times 9$  mm) as shown in Fig. 2. Four PLBs were executed for each test in the centre of the panel and of the array of sensors. Four tests were performed in total; for each one, the connections of the sensors and the channel/preamplifier pairs were swapped, so that each sensor was tested with each pair, and so any different behaviour could be related to the sensor itself rather than to the rest of the equipment. Thus for each sensor, sixteen breaks were collected.

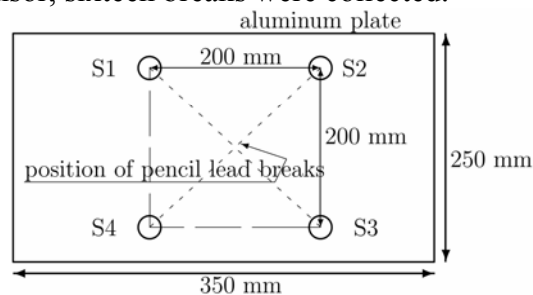


Fig. 2. Sensor positions on the aluminium plate

**Results.** Table 1 provides the average values of “absolute energy”, “duration”, “rise time”, “ring-down counts” and “amplitude” recorded from sixteen pencil lead breaks for each sensor. Table 2 displays the average frequency centroids for each sensor.

Table 1. Average values of the AE parameters

	S1	S2	S3	S4
Absolute energy [pJ]	1.017	4.721	11.300	5.782
Duration [ $\mu$ s]	13 783	16 861	20 578	19 388
Rise time [ $\mu$ s]	21	127	356	143
Ring-down counts	1 911	2 366	2 727	2 410
Amplitude [dB]	83	88	90	88

Table 2. Average frequency centroids [kHz]

S1	S2	S3	S4
325	304	377	388

**Analysis of the results and discussion.** It is immediately evident from Table 1 that, for each parameter, the values can be ordered from the highest to the lowest keeping the same order amongst the sensors, i.e. S3, S4, S2 and S1. This order is the same shown by the calibration certificates over the peaks given in region A (Fig. 1). Fig. 3 shows a power spectrum for a hit from S3 superimposed over its calibration curve. The absolute dB levels are not comparable, as the plot for the AE data has been scaled to fit on the calibration curve. It can be seen however there is close similarity in region A, a small difference in region B and a larger difference in region C, with the greatest contribution in terms of ‘energy’ coming from the lower frequencies. This goes some way to explaining why the order given in Table 1 corresponds to the order given in by the calibration certificates at the lower frequencies. There is proportionality between the duration-based parameters and the sensitivity of each sensor. Indeed, it is possible to roughly simulate the effect of a lower sensitivity with a higher threshold, as indicated by some typical data waveform shown in Fig. 4. A “new” threshold, drawn on a waveform, is obtained from the “old” (original) one by multiplication by 3.16, (i.e. 10 dB, to represent an order of magnitude of the difference in the sensitivities of the sensors). The hit duration is obtained from the last point where the waveform crosses the threshold, a reduction is observed in the duration of the same order as the difference between the durations given in Table 1 for S3 and S1, which have a 10 dB difference in sensitivity at the peak in region A. Fig. 3 shows that a PLB excites all the frequencies the sensors respond to, with a slight pre-eminence in the low frequencies. Fig. 1 shows that S2 is relatively more sensitive in the low-frequency band and less in the high-frequency one. Table 2 shows that S2 has the lowest average frequency centroid, which is to be expected as it is more sensitive in the lower frequencies. S3 and S4 give very similar average frequency centroids, which is also expected as the calibration curves from these sensors are practically identical.

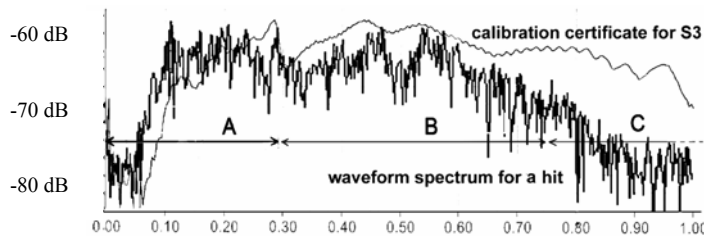


Fig. 3. A hit from sensor S3 superimposed to its calibration certificate

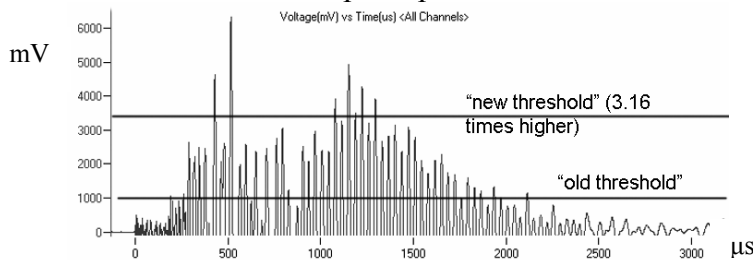


Fig. 4. New and old threshold over a half waveform

The work in this section has shown, even with simple PLB sources on isotropic media, information that is solely dependent on the source cannot be extracted from the AE parameters. In fact the parameters characterise the sensor more than the source and are highly dependent on the sensor sensitivity. For example the hit duration is related more to the measured intensity than to its length, and its dependence on the arbitrary definition of a threshold hides an equally important dependence on the unavoidable difference in the sensor sensitivities. The frequency spectra are not dependent on the sensor sensitivity as such, but are dependent on the frequency range in which the sensor is more sensitive. Therefore to carry out any form of characterisation based on either AE features or frequency spectra it is essential to use sensors that have practically identical

characteristics. To use this in any quantitative manner the sensor response needs to be calibrated accurately against a standard source.

### Effect of anisotropy and edges on the waveforms

Any real attempt to characterise a source in a composite panel must take into account that the waveforms detected by the sensors will have travelled along a heavily anisotropic medium that can possibly alter them, in a fashion that adds to the normal alterations due to wave dispersion that would also be encountered in an isotropic medium. Moreover, a panel has finite dimensions, and as such questioning any boundary effect could make sense. Any array of sensors distributed on a panel cannot know *a priori* the direction the event will come from, nor the orientation of the travelling path respect to the fibres; furthermore, a source could originate from the middle of a panel, as well as from close to the edges. In the following tests, PLBs are used to investigate the effect of the variable orientation, and proximity to the border.

**Testing setup.** Two tests were conducted in this section of work. The first test (“O”, for orientation) investigates the effect of the orientation of the fibres with respect to the travelling path. The second test (“E”, for edge) investigates the effect of the edge on the AE. In both tests S3 was placed on a [0]<sub>20</sub> 470 × 300 mm CFRP panel and connected to P3 and C3, to the PAC system. The panel was placed on a sheet of foam and then subjected to PLBs in the four positions identified as A, B, C, D in Fig. 5a for test O and as in Fig. 5b for test E and denoted as  $\alpha$ ,  $\beta$ ,  $\gamma$ ,  $\delta$ . For both tests, ten or more breaks were done for each position, but only ten were considered for the analysis, chosen from their parameters and from a visual inspection of their power spectra for the best consistency.

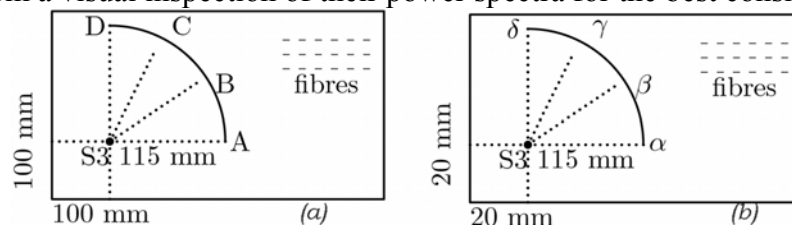


Fig. 5 Geometric configuration for test “O” and “E” (not to scale)

**Results.** The four graphs shown in Fig. 6 represent both the results from tests “O” (solid line) and “E” (dashed line). Each curve is the normalised geometric mean of ten power spectra. The scale of the vertical axis is logarithmic, whereas the abscissas represent the frequency. In tabular form, the comparison is shown in Table 3, through the average frequency centroids.

**Analysis of the results.** Results from test “O” show that the waveforms appear different when detected at a different orientation between the travelling path and the fibres. Waveforms travelling along the direction of the fibres contain some activity at higher frequencies that is lost at higher inclinations. Results from test “E” in comparison with test “O” indicate that the waveforms collected closer to the panel edges have a relatively higher high-frequency content than those collected away from the edge. The only exception seems to be the B/ $\beta$  positions, where the frequency centroid does not increase with the proximity to the border.

Table 3. Frequency centroids [kHz] of the ten events for the eight positions

	A	B	C	D
Mean	137	153	128	120
Standard deviation	27	13	25	17
	$\alpha$	$\beta$	$\gamma$	$\delta$
Mean	160	137	176	159
Standard deviation	29	24	13	17

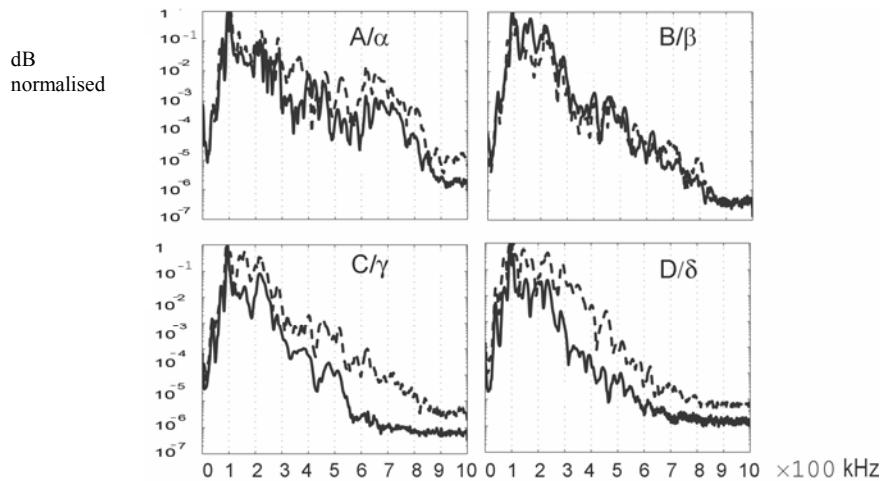


Fig. 6. Power spectra from tests “O” and “E”

### Closure

In this paper the importance of sensor consistency in terms of sensitivity and frequency response has been demonstrated. It has been shown that the AE features characterise not only the AE source but the AE measurement system as well. A case has been made for absolute calibration of sensors, however this will only be of use if the sensor response is uniform. It has been shown that an approach using frequency spectra can be adopted, which is less sensitive to the sensor response. This approach has been applied on orthotropic plates and some success has been achieved in analysing the path that a source takes through the orthotropic media.

### Acknowledgements

The authors gratefully acknowledge the support of BAE Systems.

### References

- Auld, B.A., *Acoustic fields and waves in solids*. Vol. 1. 1973: John Wiley & Sons.
- Bohse, J., *Acoustic emission characteristics of micro-failure processes in polymer blends and composites*. *Composites Science and Technology*, 2000. **60**: p. 1213–1226.
- de Groot, P.J., P.A.M. Wijnen, and R.B.F. Janssen, *Real-time frequency determination of acoustic emission for different fracture mechanisms in carbon/epoxy composites*. *Composites Science and Technology*, 1995. **55**: p. 405–412.
- Ferreira, D.B.B., et al., *Failure mechanism characterisation in composite materials using spectral analysis and the wavelet transform of acoustic emission signals*. *Insight: non-destructive testing and condition monitoring*, 2004. **46**(5): p. 282–289.
- Huguet, S., et al., *Use of acoustic emission to identify damage modes in glass fibre reinforced polyester*. *Composites Science and Technology*, 2002. **62**(10–11): p. 1433–1444.
- Johnson, M. and P. Gudmunson, *Broad-band transient recording and characterization of acoustic emission events in composite laminates*. *Composites Science and Technology*, 2000. **60**(15): p. 2803–2818.
- Johnson, M. and P. Gudmunson, *Experimental and theoretical characterization of acoustic emission transients in composite laminates*. *Composites Science and Technology*, 2001. **61**(10): p. 1367–1378.
- Mizutani, Y., et al., *Fracture mechanism characterization of cross-ply carbon-fiber composites using acoustic emission analysis*. *NDT&E International*, 2000. **33**(2): p. 101–110.
- Woo, S.-C., J.-H. Kim, and N.-S. Choi, *Fracture processes and acoustic emission in continuous fiber reinforced composite laminates*. *Key Engineering Materials*, 2004. **270-273**(111): p. 1827–1832.